IMMUNOMETABOLISM

A lipase-independent pathway of lipid release and immune modulation by adipocytes

Stephen E. Flaherty III[1]*, Ambar Grijalva[1]*, Xiaoyuan Xu[1], Eleanore Ables[1], Alireza Nomani[2], Anthony W. Ferrante Jr.[1]†

To meet systemic metabolic needs, adipocytes release fatty acids and glycerol through the action of neutral lipases. Here, we describe a secondary pathway of lipid release from adipocytes that is independent of canonical lipolysis. We found that adipocytes release exosome-sized, lipid-filled vesicles (AdExos) that become a source of lipid for local macrophages. Adipose tissue from lean mice released ~1% of its lipid content per day via exosomes ex vivo, a rate that more than doubles in obese animals. AdExos and associated factors were sufficient to induce in vitro differentiation of bone marrow precursors into adipose tissue macrophage–like cells. Thus, AdExos are both an alternative pathway of local lipid release and a mechanism by which parenchymal cells can modulate tissue macrophage differentiation and function.

In most terrestrial animals, adipocytes—which contain large, unilocular droplets of triacylglyceride (TAG) and other neutral lipids—serve as key energy storage cells. Hydrolysis of adipocyte TAG supplies substrates to meet systemic metabolic needs during periods of negative energy balance (*1*); however, in obesity and other metabolic disorders, excess lipid accumulates in cells of other tissues, including liver, skeletal muscle, and heart (*2*). Locally within adipose tissue, lipids also regulate immune cells, specifically adipose tissue macrophages (ATMs), the predominant immune cell in fat (*3*, *4*). In ATMs, accumulation of neutral lipid activates a program of lysosomal catabolism, a process that is essential for TAG hydrolysis and is associated with systemic metabolic complications, including insulin resistance and hepatic steatosis (*5*). We previously hypothesized that the neutral lipid within ATMs is generated from adipocyte-derived fatty acids that are re-esterified and incorporated in lipid droplets by ATMs. Our recent studies, however, suggest that lipid catabolism in ATM lysosomes occurs by a mechanism that is independent of autophagy (*6*). Given that autophagy is thought to be essential for lipid delivery from lipid droplets to lysosomes, an autophagy-independent mechanism in ATMs suggests that lipid destined for lysosomal catabolism may not be contained within lipid droplets (*6*).

To determine whether lipid in ATMs is localized within lipid droplets, we analyzed the expression of lipid droplet protein perilipin 2 in primary ATMs. Perilipins and related PAT family proteins associate with the phospholipid layer that covers lipid droplets (*7*). As in previous analyses and consistent with data on other macrophages, we found that perilipin 2 (*Plin2*) is the predominate PAT gene expressed in ATMs (*5*). However, confocal fluorescence microscopy of adipose tissue revealed that most lipid in ATMs does not colocalize with perilipin 2 (Fig. 1A). This contrasts with findings in foam cells—the cholesterol-laden macrophages of atherosclerotic plaques—in which a substantial portion of neutral lipid is located in lipid droplets and undergoes autophagy (*8*). Transmission electron microscopy shows that autophagolysosomes are readily apparent in foam cells, but no such structures were visible in ATMs (Fig. 1B). Lipid in ATMs appears to be stored in vesicles, distinct from the lipid droplets seen in foam cells. Given that lipid droplets form from fatty acids and glycerol in the endoplasmic reticulum during TAG synthesis, these findings suggest that accumulation of neutral lipid may not occur through a re-esterification of free fatty acids (FFAs). One possible mechanism of lipid accumulation is through endocytic uptake of intact neutral lipid.

Bone marrow cells differentiated in the presence of adipose tissue (BM-ATMs) exhibit an ATM-like phenotype with morphologic and functional characteristics typical of primary ATMs, including neutral lipid accumulation, multinuclear formation, a transcriptional profile typical of ATMs, lysosome biogenesis, and lipid catabolism (*5*, *6*). The ability of adipose

[1]Department of Medicine, Naomi Berrie Diabetes Center, Columbia University, New York, NY 07043, USA.
[2]Department of Pharmaceutics, Rutgers University, Piscataway, NJ 08854, USA.
*These authors contributed equally to this work.
†Corresponding author. Email: awf7@columbia.edu

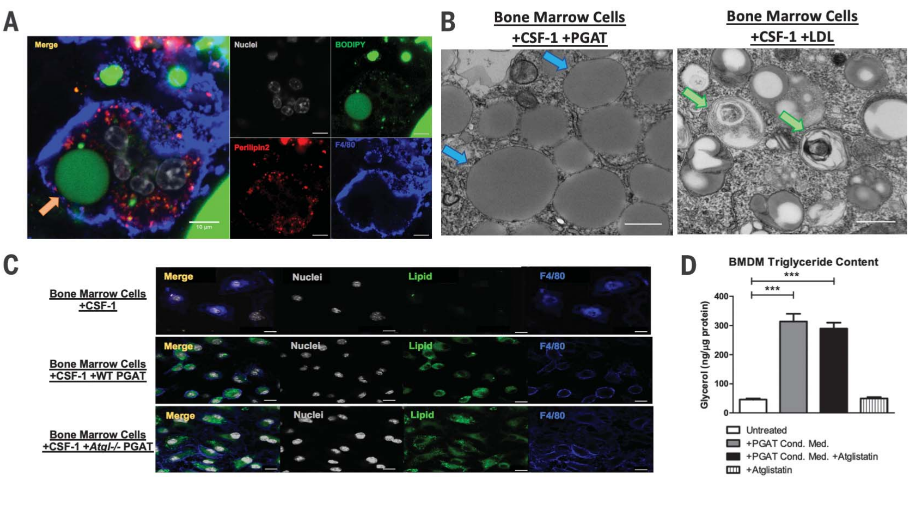

Fig. 1. Lipid accumulates in ATM lipid vesicles, independently of adipocyte ATGL activity. (**A**) Confocal microscopy images of whole PGAT from *Lep*$^{ob/ob}$ mice, immunostained with antibodies against perilipin 2 (red) and F4/80 (blue) and incubated with DNA fluorescent stain 4′,6-diamidino-2-phenylindole (DAPI) (white) and neutral lipid fluorescent stain boron-dipyrromethene (BODIPY) (green). Orange arrow highlights lipid accumulation within ATM. Scale bars, 10 μm. (**B**) Electron microscopy images of BM-ATMs (left) and bone marrow–derived foam cells (right). Arrows highlight lipid vesicles and lipid-rich autophagosomes(blue and green, respectively). Scale bars, 200 nm. LDL, low-density lipoprotein. (**C**) Confocal microscopy images of BMDMs (top), BM-ATMs differentiated in the presence of adipose tissue (middle), and BM-ATMs differentiated in the presence of *Atgl/Pnpla2*-deficient adipose tissue (bottom), immunostained with antibodies against F4/80 (blue), as well as DNA fluorescent stain DAPI (white) and neutral lipid fluorescent stain BODIPY (green). Scale bars, 10 μm. (**D**) Triglyceride content of BMDMs (untreated) or treated with medium-containing atglistatin, BM-ATM differentiated with conditioned medium of wild-type (WT) PGAT or with conditioned medium WT PGAT treated with 50 μM atglistatin. One-way analysis of variance (ANOVA); $n = 6$; ***$P < 0.001$. Error bars represent SD.

tissue to drive bone marrow cells to an ATM phenotype mirrors the ability of osteoblasts to induce osteoclast differentiation and permits analysis of factors involved in ATM development and transfer of lipid from adipocytes to macrophages. The canonical release of lipid from adipocytes requires the action of a series of neutral lipases, of which adipose triglyceride lipase (ATGL), also known as desnutrin or patatin-like phospholipase domain-containing protein 2 (PNPLA2), catalyzes the initial step (*9*, *10*). To investigate whether the canonical pathway is required for lipid accumulation in ATMs, we differentiated bone marrow cells into macrophages in the presence of adipose tissue from wild-type mice or from mutant mice deficient in ATGL (Fig. 1C). We also examined the ability of wild-type mouse adipose tissue that had been treated with an ATGL inhibitor to cause lipid accumulation in BM-ATMs (Fig. 1D). Consistent with a nonhydrolytic release of lipids, we found that the accumulation of neutral lipids in ATMs does not require adipocyte ATGL.

We next examined images of whole adipose tissue to discern whether there were any structures that might indicate the release of intact neutral lipid from adipocytes. Electron micrographs (EMs) revealed that invaginated lipid structures, consistent with the fusion or budding of smaller lipid droplets, are associated with the central lipid droplet of adipocytes (Fig. 2A). In addition, these vesicles were near structures reminiscent of multivesicular endosomes (Fig. 2A), structures typically involved in the biogenesis and release of extracellular vesicles (*11*). Together, these images and the data from ATMs prompted us to consider whether adipocytes release lipid-containing extracellular vesicles that enter an endocytic pathway in ATMs. To determine whether such adipocyte-derived vesicles exist, we cultured mouse perigonadal adipose tissue (PGAT) in the absence of serum and analyzed the conditioned medium for extracellular vesicles. EMs of adipose tissue–conditioned medium revealed a high concentration of extracellular vesicular particles ranging in diameter from 50 to 100 nm, consistent with the size of exosomes and related extracellular vesicles (Fig. 2B). Standard purification strategies for exosomes proved inefficient, possibly because of high lipid content; however, using size fractionation columns and filtration, we were able to isolate extracellular vesicles from adipose tissue. The particles contained canonical exosomal proteins (Fig. 2C),

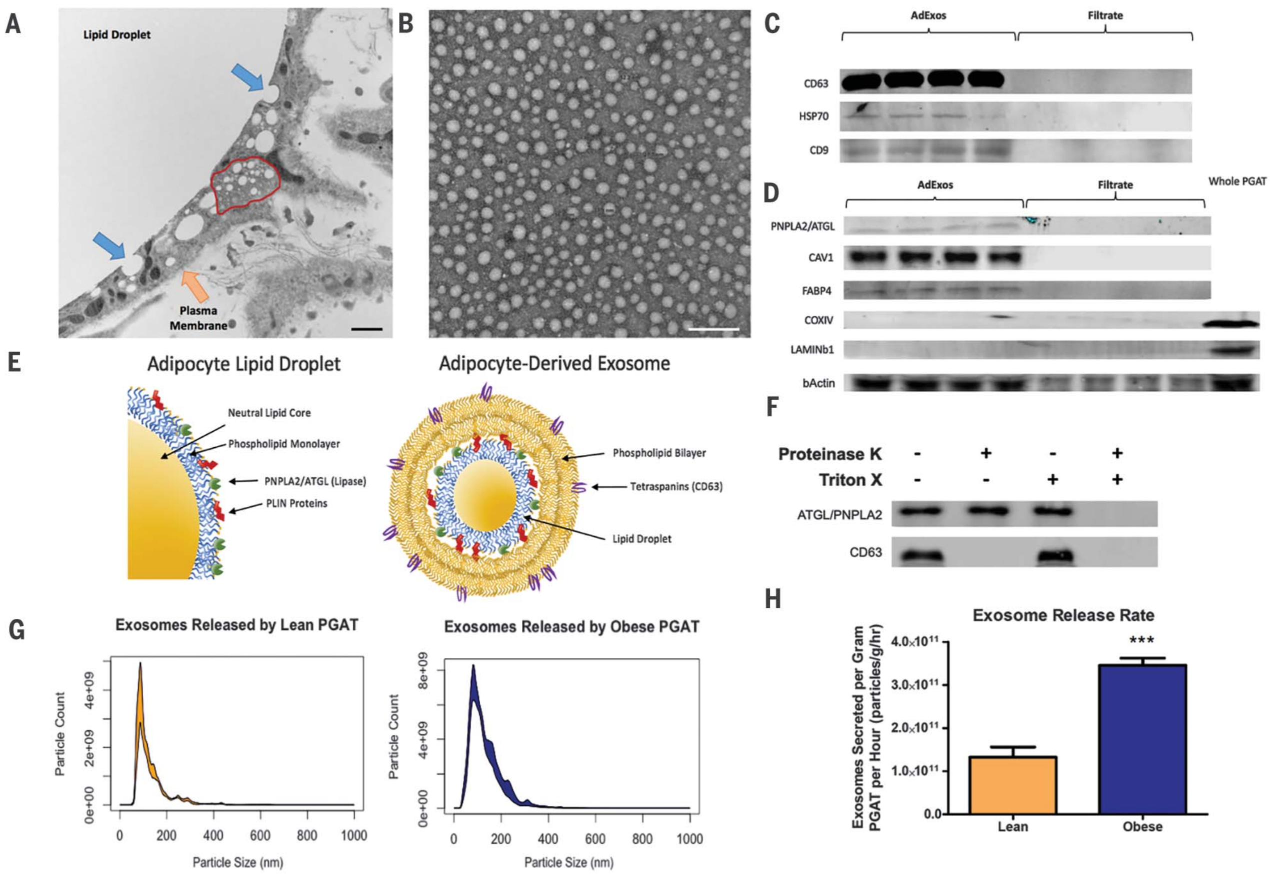

Fig. 2. Obese adipocytes release more exosomes than lean adipocytes. (**A**) Electron microscopy image of whole, fixed adipose tissue. Arrows highlight the adipocyte plasma membrane and the budding-like structures of the central lipid droplet (orange and blue arrows, respectively), and the red outline indicates a multivesicular endosome-like structure. Scale bar, 200 nm. (**B**) Electron microscopy image of vesicles collected from adipose tissue–conditioned medium. Scale bar, 200 nm. (**C**) Western blots of exosomal protein isolated from adipose tissue–conditioned media (AdExos) and conditioned media content smaller than 100 kD (filtrate). Blots were probed using antibodies against CD63, HSP70, and CD9. (**D**) Western blots of exosomal protein isolated from adipose tissue–conditioned media (AdExos), conditioned media content smaller than 100 kD (Filtrate), and whole PGAT. Blots were probed using antibodies against ATGL, CAV1, FABP4, COX4, LMNB1, and bACTIN. (**E**) Graphical representation of adipocyte lipid droplet structure (left) and hypothesized structure of adipocyte-derived exosome (right). (**F**) Western blots of protein extracted from purified exosomes that were untreated, treated with 100 μg/ml proteinase K, treated with 0.5% Triton X-100, or both. Blots were probed with antibodies against CD63 and ATGL. (**G**) Nanoparticle tracking analysis histogram of purified adipose-derived exosomes, depicting particle diameter and the number of particles at each diameter released by 1 g of lean (left, orange) or leptin-deficient obese ($Lep^{ob/ob}$) (right, blue) adipose tissue per hour. (**H**) Quantification of exosome released by adipose tissue per gram per hour from adipose tissue from lean and $Lep^{ob/ob}$ mice. Unpaired two-tailed *t* test; *n* = 8; ***P < 0.001. Error bars represent SD.

as well as adipocyte-specific proteins (Fig. 2D and fig. S1). If the invaginations seen in EM images represent budding (Fig. 2A), we predicted that any adipocyte-derived exosome would contain a lipid droplet and its associated proteins, including ATGL and PLIN1 (Fig. 2E). Consistent with this prediction, both ATGL and PLIN1 were detected in exosomes. Analysis of adipose tissue, from which ATGL had been specifically deleted in adipocytes, confirmed the adipocyte origin of the exosomal ATGL (fig. S2). We used proteinase digestion to confirm the predicted topology of the exosomes (Fig. 2E): The lipid droplet–associated protein ATGL was resistant to proteinase digestion, whereas the cytoplasmic membrane–derived protein CD63 was susceptible to it (Fig. 2F).

Combining laser light scattering microscopy with a charge-coupled device camera enables nanoparticle detection, providing accurate vesicle quantification and size estimation (*12*). Consistent with our EM images, nanoparticle tracking analysis of adipose-derived exosomes from lean C57BL/6J mice revealed that they had a mean diameter of 118 ± 57 nm (median: 102 nm). Exosomes isolated from leptin-deficient obese ($Lep^{ob/ob}$) mice had a mean diameter of 115 ± 54 nm (median: 104 nm) (Fig. 2G). PKH26, a fluorescent dye that intercalates within phospholipid bilayers, labels exosomes. When added to adipose tissue–conditioned medium, PKH26 fluorescence copurified with exosomes, as measured using nanoparticle detection (fig. S3A). In ex vivo experiments, PGAT from lean mice released, on average, 1.3×10^{11} exosomes per gram of tissue per hour, whereas PGAT from $Lep^{ob/ob}$ mice released 3.5×10^{11} exosomes g^{-1} $hour^{-1}$ (Fig. 2H). Roughly 6.0×10^{11} exosomes were released from obese tissue every 2 hours, a rate that remained constant through 12 hours in culture (fig. S3B). The number of exosomes released from adipose tissue is also acutely modulated in vivo; PGAT from fasted mice released exosomes at a rate more than twice that of adipose tissue from fed animals (fig. S4).

To confirm the adipocyte origin of these exosomes and to track them in vivo, we created a mouse line that expresses the fluorescent protein tdTomato specifically in adipocytes (AdTom) (fig. S5). Exosomes isolated from adipose tissue of these mice were fluorescent (fig. S6) and contained the tdTomato protein (Fig. 3A). The fluorescence of exosomes released from whole adipose tissue was comparable to that of exosomes released from purified AdTom adipocytes, which confirms that a majority of exosomes released from adipose tissue are adipocyte derived (Fig. 3B). Adipocyte-derived exosomes were readily detected in the blood of AdTom mice, but the ratio of CD63 to tdTomato suggested that they represent a minority of the exosomes in the circulation (Fig. 3C). This is in contrast to a recent report that the majority of circulating exosomes are adipocyte derived (*13*).

The homogeneous appearance of the centers of AdExos in EMs and the presence of lipid droplet–associated proteins suggested that AdExos contain neutral lipid. Isolated AdExos contain little FFA as compared with the total amount released from PGAT (fig. S7). In contrast, 400 mg of PGAT from a lean mouse released 980 nmol of acylglycerides per hour in exosomes (Fig. 3D), the equivalent of ~0.04% of the total acylglyceride content of the fat pad (Fig. 3E). In $Lep^{ob/ob}$ mice, the rate of lipid release increases to ~0.1% of total adipocyte acylglycerides per hour. Although these rates are dwarfed by the release of lipid during maximally activated lipolysis, a steady release rate implies the complete turnover of lipid within adipocytes every 104 days in lean animals and every 42 days in obese animals (Fig. 3E). Inhibition of lipolysis with an ATGL inhibitor reduced FFA release from adipose tissue but did not affect AdExo release (fig. S8). Through targeted lipidomics, we found that, in addition to phospholipids and free cholesterol that would be expected as part of both the lipid droplet and cytoplasmic membrane components of AdExos, adipocyte-derived exosomes contain stoichiometrically large amounts of TAGs and monoacylglycerides (fig. S9). On the basis of physical chemical properties and the concentration of TAGs and monoacylglycerides, we would predict a volume of 2.6×10^{-21} m^3 of acylglyceride per exosome. This is roughly consistent with the predicted internal volume of AdExos (derived from the measured exosome diameter) of between 1.5×10^{-21} and 7.2×10^{-21} m^3.

Lipid accumulates in ATMs with increasing adiposity (*5*) and accumulates in bone marrow cells in vitro when they are differentiated in the presence of adipose tissue (Fig. 1). To determine whether AdExos are taken up directly by ATMs within intact adipose tissue, we labeled AdExos with the fluorescent dye PKH26 and injected them into PGAT depots of lean C57BL/6J mice. Adipocytes and stromal vascular cells (SVCs) were collected from PGAT 16 hours after injection, lysed, and measured for PKH26 fluorescence. The PKH26 label was found to localize exclusively to the SVC fraction of the PGAT (Fig. 4A). This SVC fraction was further analyzed using flow cytometry, and exosome uptake was found almost exclusively (~90%) in F4/80$^+$ macrophages (Fig. 4B and fig. S10). These data demonstrate that adipocyte-released exosomes are taken up by ATMs in intact adipose tissue in vivo. Adipose tissue–conditioned medium and colony-stimulating factor 1 (CSF-1) cause lipid accumulation and differentiation of bone marrow cells into ATM-like cells. AdExos were sufficient to cause lipid accumulation in CSF-1–treated bone marrow cells (Fig. 4, C and D). Lipidomics analysis of these BM-ATMs revealed that AdExos specifically increased the TAG content of ATMs (by a factor of eight) compared with bone marrow–derived macrophages (BMDMs) not provided AdExos (Fig. 4C). Consistent with the uptake of intact TAGs, the lipid content of BM-ATMs is not dependent on fatty acid esterification via

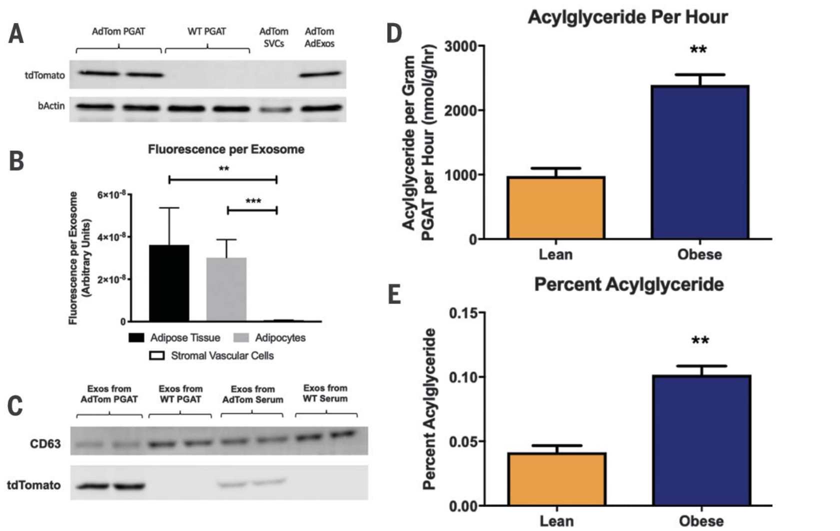

Fig. 3. Adipocyte-derived exosomes transport neutral lipid. (**A**) Western blot of total protein from whole AdTom PGAT, WT PGAT, SVCs isolated from AdTom PGAT, and AdExos isolated from AdTom PGAT. Blots were probed using antibodies against tdTomato and bActin. (**B**) TdTomato fluorescence per exosome, as measured by nanoparticle tracking analysis, for AdExos purified from whole AdTom PGAT, adipocytes isolated from AdTom PGAT, and SVCs isolated from AdTom PGAT. One-way ANOVA; $n = 4$, $^{**}P < 0.01$, $^{***}P < 0.001$. (**C**) Western blot of total protein from AdExos isolated from AdTom PGAT, AdExos isolated from WT PGAT, exosomes isolated from AdTom serum, and exosomes isolated from WT serum. Blots were probed using antibodies against CD63 and tdTomato. (**D**) Acylglyceride content of purified adipocyte-derived exosomes from lean and $Lep^{ob/ob}$ adipose tissue per gram of PGAT per hour. Unpaired two-tailed t test; $n = 8$; $^{**}P < 0.01$. (**E**) Acylglyceride content of purified adipocyte-derived exosomes, expressed as a percentage of the acylglyceride content of the tissue itself. Unpaired two-tailed t test; $n = 8$; $^{**}P < 0.01$. Error bars represent SD.

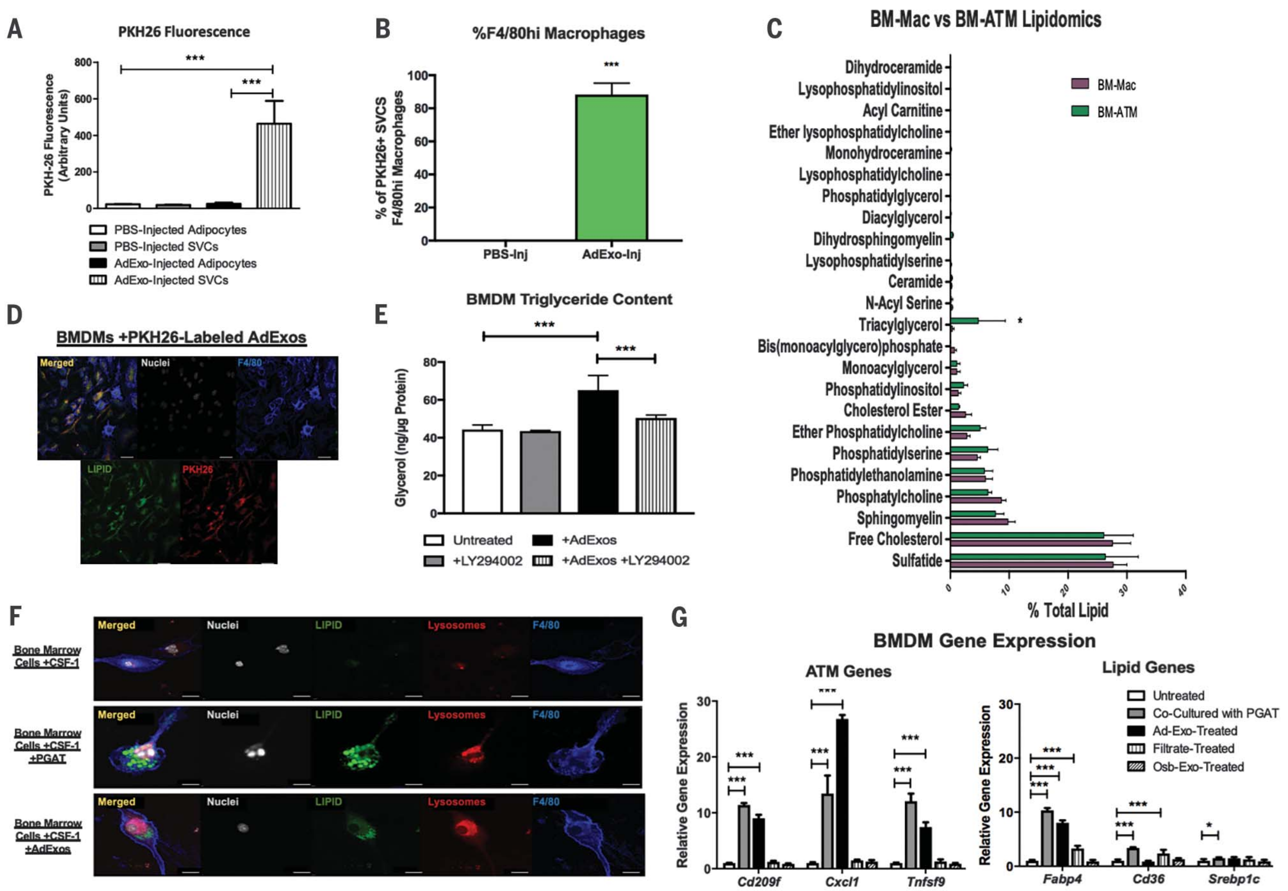

Fig. 4. AdExos are taken up by macrophages and induce an ATM-like phenotype in bone marrow cells. (**A**) PKH26 Fluorescence of adipocyte and SVC lysates from PGAT injected with phosphate-buffered saline (PBS) (left) or PKH26-labeled AdExos (right). One-way ANOVA; $n = 4$; ***$P <$ 0.001. (**B**) Percent PKH26$^+$ SVCs that are CD45.2$^+$ CD11b$^+$ F4/80hi macrophages is quantified for PBS-Inj and AdExo-Inj groups (Inj, injected), as determined by flow cytometry. Unpaired two-tailed t test; $n = 4$; ***$P <$ 0.001. (**C**) Targeted lipidomics of BMDMs cultured with (BM-ATM) or without (BM-Mac) the presence of adipose tissue. Unpaired two-tailed t test; $n = 3$; *$P < 0.05$. (**D**) Confocal microscopy images of in vitro–generated BMDMs cultured with PKH26-labeled AdExos and immunostained with antibodies against F4/80 (blue), as well as DNA fluorescent stain DAPI (white) and neutral lipid fluorescent stain BODIPY (green). Scale bars, 10 μm. (**E**) Triglyceride levels of BMDMs cultured alone, with 100 μM LY294002, with AdExos, or with both 100 μM LY294002 and AdExos for 24 hours, measured enzymatically. One-way ANOVA; $n = 6$; ***$P < 0.001$. (**F**) Confocal microscopy images of in vitro–generated BMDMs either cultured alone (top), with WT PGAT (middle), or with AdExos (bottom) for 3 days, immunostained with antibodies against F4/80 (blue), as well as DNA fluorescent stain DAPI (white), neutral lipid fluorescent stain BODIPY (green), and acidic organelle stain LysoTracker (red). Scale bars, 10 μm. (**G**) Quantitative polymerase chain reaction for BMDMs cultured alone, with WT PGAT, with AdExos, with filtrate from PGAT-conditioned medium (AdExos removed), or with exosomes secreted from primary osteoblasts (OsbExos) for 6 days. One-way ANOVA; $n = 3$ to 5; *$P < 0.05$; **$P < 0.01$; ***$P < 0.001$. Error bars represent SD.

diglyceride acyltransferases 1 and 2 (DGAT1 and DGAT2) (fig. S11), but lipid uptake is blocked by LY294002 (Fig. 4E), a phosphatidylinositol 3-kinase inhibitor that prevents macropinocytosis but does not interfere with micropinocytosis or DGAT activity.

The adipose tissue–conditioned medium from which we purify AdExos not only leads to lipid accumulation in macrophages but also induces differentiation of bone marrow progenitors into ATM-like cells, causing lysosome biogenesis and activating a transcriptional program that is characteristic of ATMs (*5*). To determine whether AdExos contribute to ATM differentiation, we treated mouse bone marrow cells with CSF-1 for 3 days and with CSF-1 and AdExos for an additional 6 days. Cells treated with AdExos accumulated lipid, became multinucleated, and displayed an increase in lysosomal content, all of which are defining features of ATMs (Fig. 4F and fig. S12). AdExos also progressively activated a transcriptional profile characteristic of ATMs, including a subset of genes previously identified as distinguishing ATMs from other tissue-resident macrophage populations (*Cxcl1*, *Tnfsf9*) but not genes associated with other tissue-resident macrophage populations, e.g., Kupffer cells (*Marco*, *Dampk*) (Fig. 4G and fig. S13). The effects of AdExos on differentiation are not a general effect of exosomes, given that exosomes from primary osteoblasts did not induce the same expression profile. Among genes involved in lipid metabolism, AdExos induced the expression of intracellular lipid–binding protein gene *Fabp4* but had no effect on the expression of the fatty acid transporter *Cd36,* whereas treatment with the filtrate (fatty acid–containing) fraction did increase *Cd36* expression in BMDMs, consistent with the disparate effects of FFA and AdExos on BMDM differentiation.

Adipocyte-derived exosomes have been described previously, primarily as regulators of inflammation and systemic insulin resistance (*13*–*18*). However, given the lipid content of the AdExos described here, it is unclear whether previous studies using standard protocols to isolate exosomes would have missed these AdExos. In this study, we found that adipocytes release lipid-laden exosomes that deliver TAG locally to macrophages and drive their differentiation. Although the systemic release of FFAs by adipocytes is part of a well-established cycle of substrate storage and release (*19*, *20*), the evidence for release of TAG by adipocytes has been scant. Locally, this pool of TAG is taken up and hydrolyzed by ATMs, establishing a local lipid cycle. The atrophy of fat depots in mice with ATMs that lack the ability to hydrolyze TAG in endolysosomes (*21*) suggests that this cycle may be important for maintaining adipose tissue homeostasis. The detection of AdExos in the circulation of mice provides a possible, previously unrecognized source of plasma triglycerides; the size and importance of this pool, however, remains to be determined.

Regulation of the tissue-specific phenotypes and functions of macrophages is not well understood. CSF-1 (and in some cases interleukin-34 and CSF-3/granulocyte-macrophage CSF) is a key regulator of differentiation of most macrophage populations (*22*), but, clearly, other signals must direct the tissue-specific development and phenotype of cells. In bone, osteoblasts are known to produce TNFSF11/RANKL, which, along with CSF-1, induces differentiation of osteoclasts (bone macrophages) (*23*). However, few other examples of local factor(s) driving tissue-specific differentiation of macrophages are known. Adipocyte-derived exosomes appear to play that role in fat and offer the possibility that a similar process may occur in other tissues. This would suggest that cellular machinery associated with the endolysosomal pathway can sense the content of exosomes and drive differentiation of macrophages to adapt and meet the needs of their local microenvironment.

REFERENCES AND NOTES

1. P. E. Scherer, *Diabetes* **55**, 1537–1545 (2006).
2. G. I. Shulman, *N. Engl. J. Med.* **371**, 1131–1141 (2014).
3. A. Kosteli *et al.*, *J. Clin. Invest.* **120**, 3466–3479 (2010).
4. E. P. Mottillo, X. J. Shen, J. G. Granneman, *Am. J. Physiol. Endocrinol. Metab.* **293**, E1188–E1197 (2007).
5. X. Xu *et al.*., *Cell Metab.* **18**, 816–830 (2013).
6. A. Grijalva, X. Xu, A. W. Ferrante Jr., *Diabetes* **65**, 967–980 (2016).
7. A. R. Kimmel, C. Sztalryd, *Annu. Rev. Nutr.* **36**, 471–509 (2016).
8. M. Ouimet *et al.*, *Cell Metab.* **13**, 655–667 (2011).
9. J. A. Villena, S. Roy, E. Sarkadi-Nagy, K. H. Kim, H. S. Sul, *J. Biol. Chem.* **279**, 47066–47075 (2004).
10. R. Zechner, P. C. Kienesberger, G. Haemmerle, R. Zimmermann, A. Lass, *J. Lipid Res.* **50**, 3–21 (2009).
11. G. Raposo, W. Stoorvogel, *J. Cell Biol.* **200**, 373–383 (2013).
12. V. Filipe, A. Hawe, W. Jiskoot, *Pharm. Res.* **27**, 796–810 (2010).
13. T. Thomou *et al.*, *Nature* **542**, 450–455 (2017).
14. Z. B. Deng *et al.*, *Diabetes* **58**, 2498–2505 (2009).
15. M. Dai, M. Yu, Y. Zhang, W. Tian, *Tissue Eng. Part A* **23**, 1221–1230 (2017).
16. E. S. Koeck *et al.*, *J. Surg. Res.* **192**, 268–275 (2014).
17. Y. Zhang, M. Yu, W. Tian, *Cell Prolif.* **49**, 3–13 (2016).
18. C. Crewe *et al.*, *Cell* **175**, 695–708.e13 (2018).
19. L. Storlien, N. D. Oakes, D. E. Kelley, *Proc. Nutr. Soc.* **63**, 363–368 (2004).
20. T. S. Nielsen, N. Jessen, J. O. Jørgensen, N. Møller, S. Lund, *J. Mol. Endocrinol.* **52**, R199–R222 (2014).
21. H. Du *et al.*, *J. Lipid Res.* **42**, 489–500 (2001).
22. E. R. Stanley, V. Chitu, *Cold Spring Harb. Perspect. Biol.* **6**, a021857 (2014).
23. H. Yasuda *et al.*, *Proc. Natl. Acad. Sci. U.S.A.* **95**, 3597–3602 (1998).

ACKNOWLEDGMENTS

We thank E. Kershaw for *Atgl*-floxed mice, and K. Brown, R. Chan, G. Di Paolo, P. Petropoulou, S. Kousteni, H. Ginsberg, S. Ramakrishan, and A. Hatefi for technical assistance and advice. **Funding:** The authors acknowledge NIH grants R01DK066525, P30DK026687, P30DK063608, and T32DK007328, and support from the Russell Berrie Foundation. **Author contributions:** A.W.F. and S.E.F. developed the research strategy and experimental designs; S.E.F., A.G., E.A., X.X., and A.N. performed the experiments; A.W.F. coordinated all activities; A.W.F. and S.E.F. prepared the figures and wrote the manuscript. All authors approved the final manuscript. **Competing interests:** The authors declare no competing interests. **Data and materials availability:** All data are available in the manuscript or the supplementary materials.

SUPPLEMENTARY MATERIALS

www.sciencemag.org/content/363/6430/989/suppl/DC1
Materials and Methods
Figs. S1 to S13
Table S1
Reference (*24*)

3 December 2018; accepted 11 January 2019
10.1126/science.aaw2586

Science

A lipase-independent pathway of lipid release and immune modulation by adipocytes

Stephen E. Flaherty III, Ambar Grijalva, Xiaoyuan Xu, Eleanore Ables, Alireza Nomani and Anthony W. Ferrante Jr.

Science **363** (6430), 989-993.
DOI: 10.1126/science.aaw2586

Exosomes that fatten immune cells

Adipose tissue in mammals contains not only adipocytes (fat cells) but also a variety of immune cells––most notably, macrophages. Proper communication between these cell types is thought to be important for metabolic health. Flaherty *et al.* found that adipocytes release lipid-filled vesicles (AdExos) that serve as the primary source of lipid for adipose-resident macrophages (see the Perspective by Antonyak *et al.*). AdExos were present at low levels in the circulation of mice and were produced at twice the rate in obese versus lean animals. In vitro, AdExos induced differentiation of bone marrow precursor cells into cells resembling adipose-resident macrophages.

Science, this issue p. 989; see also p. 931

Science (print ISSN 0036-8075; online ISSN 1095-9203) is published by the American Association for the Advancement of Science, 1200 New York Avenue NW, Washington, DC 20005. The title *Science* is a registered trademark of AAAS.